W.H. LEE[*,♯], Y.J. JO[*], Y.H. KIM[**], Y.H. JO[*], J.G. SEONG[*], C.J. VAN TYNE[***], S.Y. CHANG[****]

SELF-CONSOLIDATION MECHANISM OF POROUS TI-6AL-4V IMPLANT PROTOTYPES PRODUCED BY ELECTRO-DISCHARGE-SINTERING OF SPHERICAL TI-6AL-4V POWDERS

MECHANIZM AUTOKONSOLIDACJI PROTOTYPÓW POROWATYCH IMPLANTÓW WYTWORZONYCH PRZEZ SPIEKANIE SFERYCZNYCH PROSZKÓW Ti-6Al-4V

Electro-Discharge-Sintering (EDS) was employed to fabricate Ti-6Al-4V porous implant prototypes from atomized powders (100 - 150 μm), that were subjected to discharges of 0.75 to 2.0 kJ/0.7g-powder from 150, 300, and 450 μF capacitors. Both fully porous and porous-surfaced Ti-6Al-4V compacts with various solid core sizes were self-consolidated in less than 86 - 155 μsec. It is known that EDS can simultaneously produce the pinch pressure to squeeze and deform powder particles and the heat to weld them together. The formation of a solid core in these prototypes depends on the amounts of both the pinch pressure and heat generated during a discharge. The size of the solid core and the thickness of the porous layer can be successfully controlled by manipulating the discharge conditions such as input energy and capacitance.

Keywords: Ti-6Al-4V, implant, porous, sintering, electro-discharge

1. Introduction

The desired surface features of dental or orthopedic implants have changed from smooth to notched surfaces. Most implants are presently designed to maintain immobility during healing so that osseointegration will occur. One of the proposed designs, a porous-coated implant, is intended to increase the surface area for the promotion of immobilization of the implant in the bone by enabling mechanical interlocking between the implant and tissue, which can lead to faster osseointegration [1-4].

The fabrication of porous-coated Ti based implants normally involves either plasma-spraying or sintering powders onto a solid substrate [5-8]. The usual sequence of powder metallurgy operations is to compact a metal powder in a die at room temperature and subsequently sinter it at elevated temperatures. Not only are high pressures, high temperatures, and long times required, but for reactive materials, such as Ti and its alloys, an inert atmosphere is also required.

Fully porous Ti implants (no solid core) and porous-surfaced implants with a core were fabricated and mechanically tested by Asaoka *et al.* [6]. Ti powders packed in an alumina mold were sintered in a vacuum at 1000°C for 24 hours. The resulting Ti compact revealed rather weak bonding. The pre-sintered compact was further sintered in a vacuum without the mold for 24 hours at 1400°C. A Ti rod inserted into an alumina mold served as a solid core, and Ti powder was used to fill the space surrounding the core. Sintering was performed under the same conditions as those employed for the fully porous Ti specimens. The resulting compressive strengths of implant prototypes were in the range of 184-237 MPa, depending on the solid core size. The microstructure showed a typical large grained α and β structure both in the core and in the porous regions of the implant.

Dewidar and Lim have also tested properties of porous-surfaced Ti-6Al-4V implants manufactured by conventional powder metallurgy [5]. The compressive yield strengths for the specimens with 30, 50, and 70% porosity were in a range of 150-270 MPa. The strength depended significantly on both the core size and the porosity of the surface. Typical large-grained α and β structures in both the core and porous portions of the implant were observed in the microstructure. The grain growth, phase transformation, and low yield strength is somewhat inevitable due to an exposure at high temperature for a long time.

To overcome these problems, which are related to the high temperature sintering process for the fabrication of porous-surfaced Ti implant prototypes, we have introduced electro-discharge-sintering (EDS) which uses a high voltage and a high current pulse [9-12]. Fully porous and porous-surfaced Ti-6Al-4V implant prototypes without a change of microstructure were produced by EDS of Ti-6Al-4V spherical powders. The size of solid core and the thickness of porous layer can be successfully controlled by the discharge conditions.

*   SEJONG UNIVERSITY, FACULTY OF NANOTECHNOLOGY AND ADVANCED MATERIALS ENGINEERING, SEOUL 143-747, SOUTH KOREA
**   WONKWANG HEALTH SCIENCE UNIVERSITY, DEPARTMENT OF DENTAL LABORATORY TECHNOLOGY, IKSAN 570-750, SOUTH KOREA
*** COLORADO SCHOOL OF MINES, DEPARTMENT OF METALLURGICAL AND MATERIALS ENGINEERING, GOLDEN 80401, USA
**** KOREA AEROSPACE UNIVERSITY, DEPARTMENT OF MATERIALS ENGINEERING, GOYANG-SI 412-791, SOUTH KOREA
♯   Corresponding author: whlee@sejong.ac.kr

The mechanism of self-consolidation of the porous-surfaced Ti-6Al-4V implant prototypes by EDS, however, has not yet been explained in detail. This paper analyzes the electro-discharge characteristics in terms of input energy, capacitance, and discharge time. It also systematically describes the means by which the electro-discharge consolidates the Ti-6Al-4V powder particles to produce porous-surfaced compacts having a solid core.

2. Experimental procedure

The spherical Ti-6Al-4V powders were produced by electrode-induction-melting gas atomization. They were sieved to yield a single particle size class of 100 - 150 μm. A sample of 0.7 g of the powder was vibrated into a quartz tube with an inner diameter of 4.0 mm that was equipped with tungsten electrode at the top and bottom. A copper heat sink tube was placed into the quartz mold. The discharging chamber was evacuated to 2×10^{-3} torr and then filled with Ar gas at 1000 torr. Three different capacitor banks (150, 300 and 450 μF) were charged with four different electrical input energies (0.75, 1.0, 1.5 and 2.0 kJ). The charged capacitor bank instantaneously discharged through the powder column by an on/off high vacuum switch which closed the discharge circuit. The voltage and the current that the powder column experienced when the circuit was closed were simultaneously measured by a high-voltage probe and a high-current probe, respectively. Outputs from these probes were fed into a high-speed oscilloscope that stored them as a function of discharge time. The overall process is referred to as electro-discharge-sintering (EDS). Figure 1 shows a schematic of the EDS apparatus.
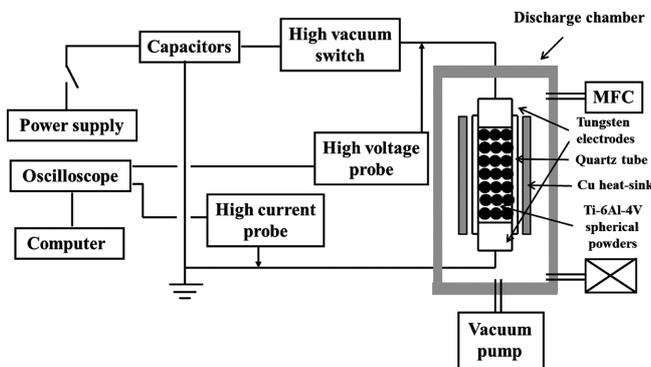
Fig. 1. Electro-discharge-sintering schematic

Each EDS implant compact was sliced every two millimeters, and the resulting cross-sections were examined under an optical microscope and a scanning electron microscope (SEM). The effects of discharge condition on the porosity of EDS compacts were investigated. Finally, a self-consolidation mechanism for a fully porous and a porous-surfaced implant compacts produced by EDS is proposed.

3. Results and discussion

A typical discharge curve (Fig. 2(a)) shows voltage and current in terms of discharge time. 450 μF of capacitance and 2.58 kV of input voltage were employed to yield 1.5 kJ with the implant having a particle size of 100 - 150 μm. This figure shows that the peak current is 17.5 kA and the peak voltage is 2.0 kV. From Fig. 2(a), a power (W) curve is plotted in Fig. 2(b) against the discharge time. The power increases with an increase in input energy at constant capacitance. The discharge times for the duration of the first cycle at the conditions of 150, 300, and 450 μF of capacitance were approximately 89, 125 and 156 μsec, respectively. The duration of discharge strongly depends on the capacitance. The amount of heat (ΔH) generated during a discharge can be obtained approximately by:

$$\Delta H = \Sigma[I^2(t)R(t)\Delta t] \quad (1)$$
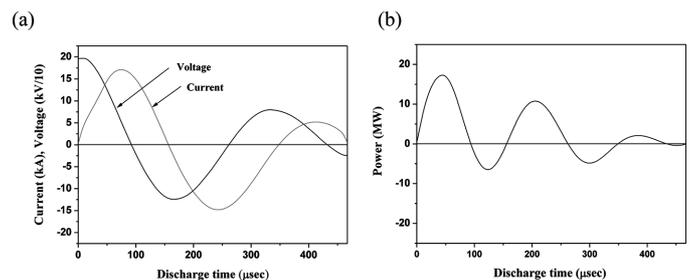
Fig. 2. (a) Typical discharge curve of measured current and voltage recorded on an oscilloscope and (b) typical power curve versus discharge time (discharge condition: 450 μF, 1.5 kJ)

Table 1 gives the amounts of heat generated for each experimental condition. It is seen that ΔH increases with an increase in input energy at constant capacitance.

TABLE 1

Peak current, current density (j), heat generated (ΔH), maximum temperature, and pinch pressure (P) produced by a discharge under various EDS conditions

Capacitance (μF)	Input energy (kJ)	Peak current (kA)	Current density (A/m^2)	ΔH (J)	Max. temp. (°C)	Pinch pressure (MPa)
150	0.75	11.6	1.54×10^{11}	640	1377	12
150	1.0	14.8	1.96×10^{11}	891	2020	19
150	1.5	16.8	2.22×10^{11}	1263	2969	25
150	2.0	20.4	2.70×10^{11}	1677	4025	37
300	0.75	11.2	1.48×10^{11}	564	1186	11
300	1.0	13.6	1.80×10^{11}	846	1905	16
300	1.5	17.6	2.33×10^{11}	1445	3433	27
300	2.0	20.0	2.65×10^{11}	1874	4527	35
450	0.75	10.4	1.38×10^{11}	515	1058	10
450	1.0	13.2	1.74×10^{11}	849	1912	15
450	1.5	17.6	2.33×10^{11}	1465	3484	27
450	2.0	20.4	2.70×10^{11}	1962	4752	37

Figure 3 shows the EDS implant compact after a discharge, illustrating a typical porous surface. The porosities of the compacts fabricated at a constant capacitance of 300 μF with varying input energy range from 40.3% to

23.3%. The porosity decreases with an increase in input energy. Figure 4 shows optical micrographs that illustrate typical cross-sectional views of EDS implant compacts fabricated with two different input energies. Figure 4(a) shows that a fully porous compact throughout the cross-section can be obtained without forming a solid core. However, using an input energy greater than 1.0 kJ produces a solid core in the center of the compact which is surrounded by a porous layer (Fig. 4(b)). The solid core is composed of Ti-6Al-4V powder particles that were deformed and welded together. The porous layer consists of powder particles that were connected by necks in three dimensions, although only one-dimensional necks are observed on the polished plane.
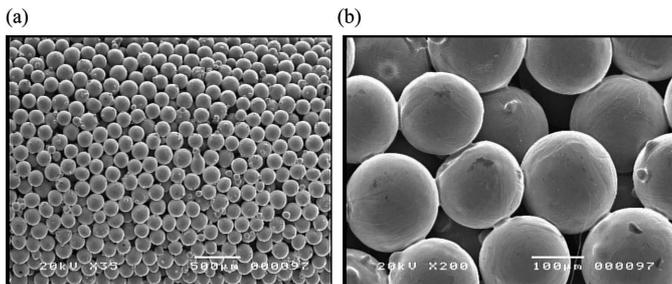
Fig. 3. (a) Typical EDS compact and (b) magnified from Fig. 4(a) (discharge condition: 300 μF, 1.5 kJ)
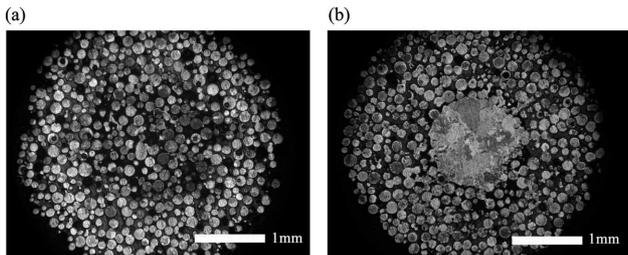
Fig. 4. Cross-section view of an EDS compact discharged at (a) 0.75 kJ and (b) 1.0 kJ with a capacitance of 300 μF

Figures 5(a) and 5(b) show typical optical micrographs of powder particles in the porous layer and the solid core of the EDS compact, respectively. Both the solid core and powder particles in the porous layer exhibited a typical Widmanstätten $\alpha + \beta$ structure. The lamellae spacing is very fine, which is a characteristic of atomized Ti-6Al-4V powders produced at a high cooling rate, as reported by Eylong and Froes [13]. Therefore, EDS does not change the unique microstructure of the Ti-6Al-4V powder.
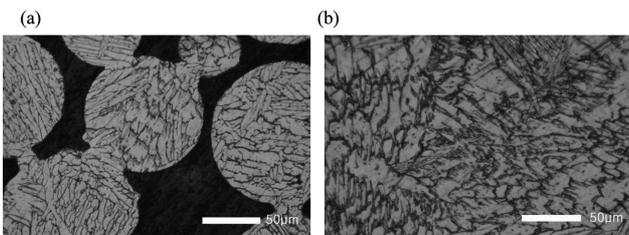
Fig. 5. Typical optical micrographs of (a) powders in the porous layer and (b) the solid core of the compact (discharge condition: 150 μF, 1.5 kJ)

The average solid core size was measured. The core increased from 0 to 3.9 mm with increased input energy at constant capacitance. Since EDS should require enough heat to weld powder particles together, similar to a conventional powder metallurgy process, the solid core sizes are plotted against the heat generated (ΔH). Figure 6 shows that all the data points are well aligned along a straight line, except for the discharge conditions with ΔH less than 0.75 kJ. In this low heat condition, no solid core was formed.
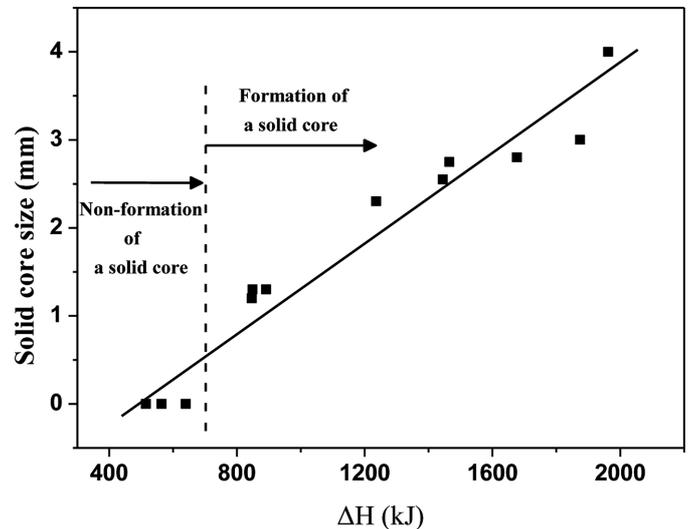
Fig. 6. Solid core size versus heat generated (ΔH)

To understand the effect of ΔH on the formation of a solid core, two important parameters, which are closely related to the current density, need to be considered. First, the temperature rise (ΔT) at the powders' interface, which is generated by the input energy, is considered and then estimated from:

$$W = mCp\Delta T \qquad (2)$$

where m is the mass of Ti-6Al-4V powder and Cp is the specific heat of Ti-6Al-4V [14]. The electrical input power (W) was calculated by integrating the current and voltage as a function of discharge time. Table 1 lists the maximum temperatures (ΔT – 25°C) generated through the powder particles by EDS under various discharge conditions. It is noted that the EDS process using 0.75 kJ of input energy at three different capacitances produced maximum temperatures through the powder particles in the range from 1058°C to 1377°C. In contrast, using input energies more than 1 kJ the maximum temperature is higher than the melting temperature of Ti-6Al-4V. These heat levels are high enough to form the necks between powder particles, even for the very short times such as 86 - 156 μsec. However, the heat during a discharge alone cannot fully explain the formation mechanism of solid core in the middle of the implant compact, since no external pressure was applied to the powder column during EDS. Therefore, the formation of a solid core should be related to the mechanical force generated during a discharge.

When a capacitor bank is discharged through a powder column confined in a tube, a long cylindrical metal powder column conducting a current density tends to contract radially inward. At this moment, the magnetic field generated by the current flow causes a diametrical contraction, which is known as the pinch effect [15]. The resulting pinch pressure is the

mechanical force acting on the powder column that produces a solid core. The pinch pressure (P) is given by:

$$P = \mu j^2 (a^2 - r^2)/4 \qquad (3)$$

where μ is the permeability, j is the current density, a is the radius of the cylindrical conductor, and r is the distance from the center of the powder column where pressure P is calculated. The diameter, $2a$, of the contact region is approximately one-tenth of the diameter of an average powder particle, as is often the case in solid mechanics calculations [16]. The maximum pinch pressure can be estimated in the center of the contact area (at $r = 0$). In practice, spherical powders readily arrange themselves in a close-packed manner. This arrangement causes that the pinch pressure to be one-ninth of the estimated value [14]. Table 1 also lists resulting pinch pressures calculated under various EDS experimental conditions.
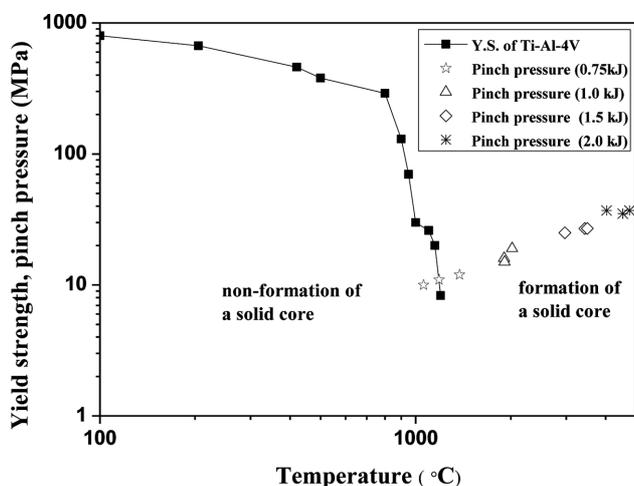
Fig. 7. Temperature dependence of yield strength of Ti-6Al-4V and pinch pressure and heat generated during an electro-discharge-sintering (discharge condition: 300 μF)

The EDS process can produce both the pinch pressure and heat simultaneously. The pinch pressure as a mechanical force will push the Ti-6A-4V powder particles together, and deforms them to create an aggregate. Figure 8 shows the yield strength of Ti-6Al-4V as a function of temperature. The pinch pressure versus maximum temperature generated by a discharge under current EDS conditions are also plotted. For the discharge conditions with an input energy of 0.75 kJ at three different capacitances, the pinch pressure range from 10 to 12 MPa while maximum temperature is between 1058°C and 1377°C. These pressures are just above the value of yield strength of Ti-6Al-4V at the corresponding temperature. A relatively low pinch pressure results in only the neck formation between powder particles, and the pressure is insufficient to create a solid core. Using an input energy more than 1 kJ, the heat through the powder particles is much higher, and as a result, the Ti-6Al-4V powder particles are easily deformed and consolidated into the form of solid bulk with the aid of the pinch pressure (15 - 37 MPa) in a time as short as 86 - 156 μsec.

Figure 8 shows a plot of the distribution of the estimated pinch pressure applied through the cross-section of an EDS compact. The pinch pressure decreases to 0 at the surface.

Since the pinch pressure is a maximum at the center of the powder column, the solid core is formed easily, especially in the middle of an EDS compact, producing a porous-surfaced structure with a solid core.
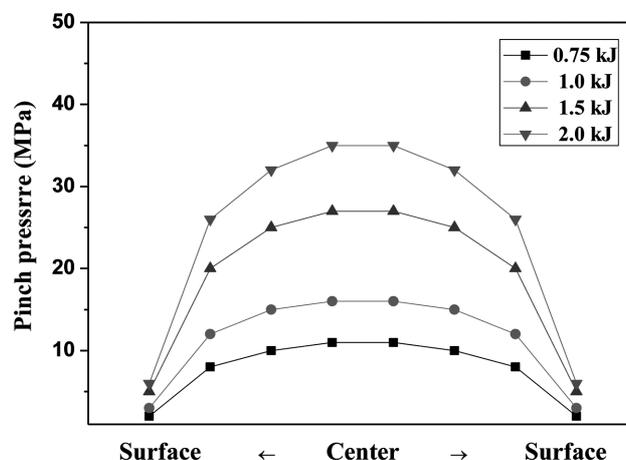
Fig. 8. Distribution of pinch pressure generated through the cross-section of EDS compact (discharge condition: 300 μF)

In conclusion, the formation of a solid core in the middle of EDS compact by a discharge requires both the pinch pressure to squeeze and deform powder particles and heat to weld them together. The amount of pinch pressure and heat are closely related to ΔH. It is thus suggested that capacitance and input energy are controllable discharge parameters for the self-consolidation of fully porous and porous-surfaced Ti-6Al-4V implant compacts fabricated by EDS.

4. Conclusions

Fully porous and porous-surfaced Ti-6Al-4V implant compacts were self-consolidated by electro-discharge-sintering (EDS) of atomized spherical powders in times as short as 86 - 155 μsec. In the case of the porous-surfaced compact, the solid core was composed of acicular grains with a Widmanstätten $\alpha + \beta$ structure of Ti-6Al-4V alloy, and the porous layer consisted of particles connected in three dimensions by necks. EDS is able to simultaneously produce both the pinch pressure to squeeze and deform powder particles and the heat to weld them together. With a sufficient rise in heat, the pinch pressure can push the Ti-6A-4V powder particles together and deform them to create aggregates, which results in the formation of a solid core. It is thus suggested that capacitance and input energy are controllable discharge parameters affecting the amount of pinch pressure and heat for the self-consolidation of porous-surfaced Ti-6Al-4V implant compacts by EDS.

REFERENCES

[1] D. Deporter, R. Todescan, P. Watson, M. Pharoah, R.M. Pilliar, G. Tomlinson, Int. J. Oral Maxillofacial Implants **16**, 527 (2001).

[2] D. Deporter, R.M. Pilliar, R. Todescan, P. Watson, M. Pharoah, Int. J. Oral Maxillofacial Implants **16**, 653 (2001).

[3] H.Q. Nguyen, D. Deporter, P.M. Pilliar, N. Valiquette, R. Yakubovich, Biomater. **25**, 865 (2004).

[4] V. Amigo, M.D. Salvador, F. Romero, C. Solves, J.F. Moreno, J. Mater. Proces. Technol. **14**, 117 (2003).

[5] M.M. Dewidar, J.K. Lim, J. Alloys Comp. **454**, 442 (2008).

[6] K. Asaoka, N. Kuwayama, O. Okuno, I. Miura, J. Biomed. Mater. Res. **19**, 699 (1985).

[7] S. Yue, R.M. Pillar, G.C. Weatherly, J. Biomed. Mater. Res. **18**, 1043 (1984).

[8] R.M. Pilliar, J. Biomed. Mater. Res. **21**, 1 (1987).

[9] H.S. Jang, Y.J. Cho, T.J. Kang, K.B. Kim, W.H. Lee, J. Kor. Inst. Metals Mater. **47**, 488 (2009).

[10] Y.W. Cheon, N.H. Oh, Y.H. Kim, C.S. Byun, S.H. Lee, W.H. Lee, J. Kor. Powd. Met. Inst. **12**, 1 (2005).

[11] Y.W. Cheon, Y.J. Cho, T.J. Kang, J.Y. Kim, J.S. Park, C.S. Byun, S.H. Lee, W.H. Lee, J. Kor. Inst. Metals Mater. **47**, 660 (2009).

[12] Y.J. Cho, Y.H. Kim, Y.H. Jo, M.J. Kim, H.S. Kim, S.W. Kim, J.H. Park, W.H. Lee, J. Kor. Powd. Met. Inst. **20**, 376 (2013).

[13] D. Eylong, F.H. Froes, Symposium on Titanium Rapid Solidification Technology, F.H. Froes and D. Eylong (eds.), AIME, Warrendale 1986.

[14] D.K. Kim, H.R. Pak, K. Okazaki, Mater. Sci. Eng. A **104**, 191 (1988).

[15] M. Shakery, S. Al-Hassani, T.J. Davies, Powd. Metall. Int. **11**, 120-125 (1970).

[16] T.H. Wu, Solid Mechanics, Alleyn and Bacon, Boston 1976.